Reaction temperature-dependent growth of ZnS nanomaterials

Chang Liu, Xiang Wu ✉

School of Materials Science and Engineering, Shenyang University of Technology, Shenyang 110870, People's Republic of China
✉ *E-mail: wuxiang05@163.com*

Published in Micro & Nano Letters; Received on 7th July 2017; Revised on 7th August 2017; Accepted on 1st September 2017

Zinc sulphide (ZnS) nanobelts and nanotubes with high yield are prepared by a simple chemical vapour deposition approach at different reaction temperature. The as-prepared products are characterised by several characterisation methods such as X-ray diffraction, scanning electron microscopy, transmission electron microscopy, Raman spectrum and photoluminescence spectrum. It shows that the as-prepared ZnS products possess well-hexagonal wurtzite structures. Possible growth mechanisms of ZnS nanomaterials are proposed based on nucleation and oriental attachment. Photoluminescence spectrum of ZnS nanobelts shows a blue emission peak centred at 425 nm, which could be attributed to the defects associated with oxygen vacancies. Finally, the wettability of ZnS nanobelts is also investigated by water contact angle characterisation.

1. Introduction: As an important II–VI semiconductor material, zinc sulphide (ZnS) has been a hotspot of scientific research because of its unique physical and chemical properties [1–5]. Particularly, prominent feature with wide bandgap energy (3.68 eV) of ZnS presents excellent performance of luminescence and photochemistry [6–9]. One-dimensional (1D) nanoscale ZnS structures with controllable morphologies and sizes have attracted one's attention in recent two decades due to their unique geometric structures and large aspect ratios. 1D nanostructures including nanowires, nanotubes, nanorods and nanobelts are widely investigated because of the fascinating fundamental properties and potential applications in various fields [10, 11] such as electrode materials [12–14], luminescent devices [15, 16] and gas sensors [17].

Among various preparation methods, Chemical vapor deposition (CVD) synthesis owns good advantages of simple operation, high crystal quality. Herein, ZnS nanobelts and nanotubes with high yield are prepared using a simple CVD process without adding any metal catalysts and the templates. Growth mechanisms of the as-synthesised ZnS products are proposed. Photoluminescence spectrum of ZnS nanobelts at room temperature shows a strong green emission at 525 nm. Contact angle of 113° of ZnS nanobelts suggests its hydrophilic characteristic.

2. Experimental section: The sample was synthesised by a facile CVD process. High-purity mixture of ZnS and a trace of C power were put in an alumina boat located at the centre of a tube furnace. Silicon (Si) substrates covered with gold (Au) film were placed at downstream away from alumina boat about 7 cm. After evacuating the quartz tube, pure argon gas flow was introduced into the furnace by a flow of 50 sccm, where reaction temperature was kept at 1200 and 1300°C for 30 min, respectively. After reaction finished, the furnace was naturally cooled to room temperature.

The morphology, crystal structure and composition of the as-grown nanostructure were characterised with X-ray diffraction analyser (XRD, Rigaku Dmax-rB, CuK α radiation, $\lambda = 0.1548$ nm, 40 kV, 100 mA), scanning electron microscopy (SEM, Hitachi S-4800), transmission electron microscopy (TEM, JEOL-2010) and energy dispersive X-ray spectrum (EDS) and microlaser Raman spectroscope (HR800). Optical properties and wetting behaviours of ZnS nanobelts were investigated by photoluminescence spectroscopy (PL SPEX FL-2T2) and a contact angle (CA) system (KINO SL200 B) at room temperature.

3. Results and discussion: To identify crystal structure of the as-synthesised product, XRD analysis is performed and the

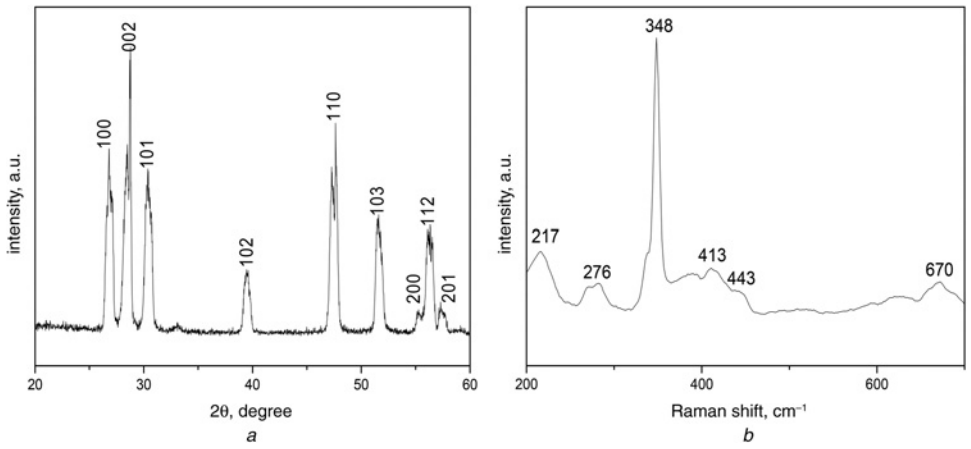

Fig. 1 *Crystal structure of the as-synthesised product*
a XRD pattern of the as-prepared products
b Raman spectrum of the as-prepared products

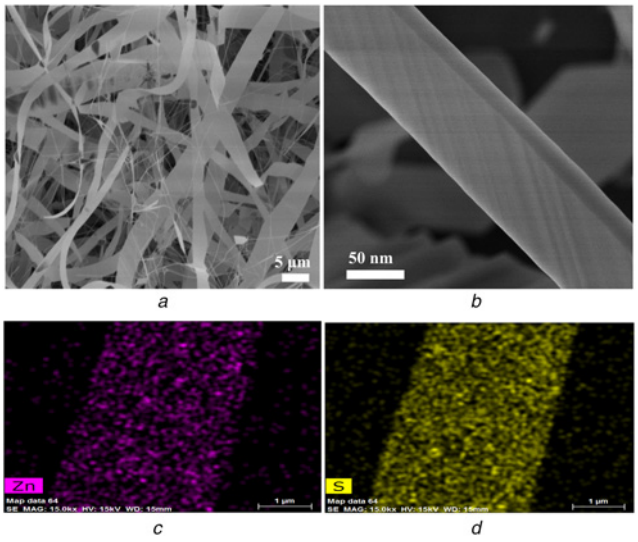

Fig. 2 *Morphology of the as-prepared product*
a, b Different magnification SEM images of the as-prepared products
c, d EDS mapping images

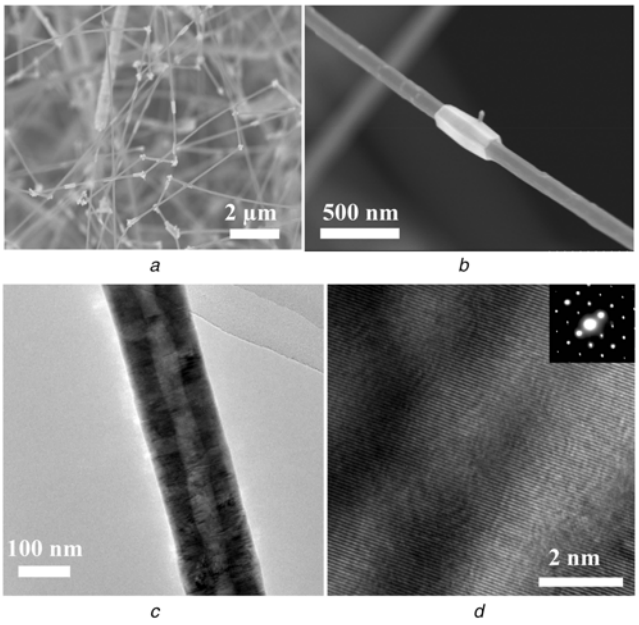

Fig. 3 *Morphology of the as-prepared ZnS nanotubes at 1300°C*
a, b SEM images of the as-prepared ZnS nanotubes
c, d TEM images of the as-prepared ZnS nanotubes

corresponding pattern is shown in Fig. 1*a*. The observed result shows that all the diffraction peaks are well-identified with hexagonal wurtzite ZnS with lattice constants of $a = 0.382$ nm and $c = 0.627$ nm, which is well-matched with the literature values (standard PDF Card No. 36-1450) [18]. There are no other impurity peaks appearing, indicating that the product possesses high purity. Furthermore, strong well-defined diffraction peaks confirm well-crystallinity of ZnS product. Raman spectrum of the as-synthesised ZnS product is showed in Fig. 1*b*. Main peak centred at 348 cm^{-1} could be attributed to ZnS lattice vibration in ZnS. Rest of the peaks at 217, 276, 413, 463 and 670 cm^{-1} are in accordance with standard ZnS phase [19]. Raman spectrum feature of the as-prepared ZnS product confirms their typical wurtzite structures.

The morphology of the as-prepared product is examined by SEM, as shown in Fig. 2*a*. It can be found the as-synthesised product presents large quantity of nanobelt-like shape. Further observation finds that the nanobelt possesses an average thickness of ~5 nm, as shown in Fig. 2*b*, confirming the thickness of the nanobelt is very thin. To identify chemical composition of the as-synthesised product, EDS elemental analysis is studied and the corresponding spectrum is presented in Figs. 2*c and d*. It obviously shows the presence of only Zn and S elements with near equal ratio.

To study effect of reaction parameter on morphology of the as-synthesised ZnS products, temperature-dependent experiment is conducted. When kept 30 min of reaction time unchanged, we increase reaction temperature to 1300°C. Surprisingly, wire-like nanostructure forms. Fig. 3*a* shows low magnification SEM images of the as-prepared products, further observation finds each nanowire has a knot coating on the surface. TEM image of the as-prepared product proves the wire present tube-like shape. High-resolution TEM image as shown in Fig. 3*d* reveals the well-defined lattice fringes with lattice spacing of 0.31 nm, which corresponds to (001) lattice plane of ZnS. It suggests that temperature can exert important influence on final morphology of the as-synthesised products.

On the basis of above experimental results, a possible growth mechanism for ultrathin ZnS nanobelt can be proposed. At early stage of reaction, ZnS powder is evaporated into ZnS vapour and flows downwards to nucleate on Si deposition substrate by carrier gases. Nucleation process is affected seriously due to surface energy driving and thermodynamics instability. With the reaction proceeding, ZnS nucleates quickly to continue crystal growth, which is caused by minimising surface energy of the orientation. Then, the aggregated nanoparticles combine with each other to form nanobelt-shaped morphology due to anisotropic growth. Meanwhile, the length of the nanobelt becomes longer and the thickness becomes ultrathin.

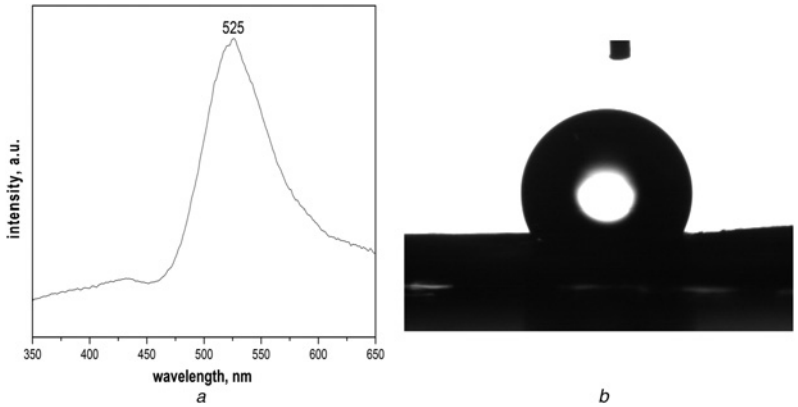

Fig. 4 *Photoluminescence of ZnS nanobelts*
a Room temperature PL spectrum of the as-prepared ZnS nanobelts
b Contact angle photograph of the as-prepared ZnS nanobelts

doi: 10.1049/mnl.2017.0492

Photoluminescence of ZnS nanobelts is investigated at room temperature and the spectrum is shown in Fig. 4*a*. Obviously, a broad, strong green emission peak centred at 525 nm is detected. Zhang *et al.* thought that green emission at 520 nm from ZnS nanowires originates from Au impurity [3]. However, in our experiments, there are not any catalysts used. We think it can be attributed this peak to ZnS self-activated centre.

Finally, we also study the wettability of the as-synthesised ZnS nanobelts, CA photographs of ZnS nanobelts are shown in Fig. 4*b*, revealing that the as-obtained ZnS nanobelts are hydrophobic with 113° contact angle. It is the case that surface free energy and geometric construction of the product play very important roles in wetting behaviour. Generally speaking, hydrophobic materials own low surface free energy and large surface roughness [20]. Surface roughness of as-synthesised ZnS nanobelts may arouse water CA large, demonstrating potential application in self-cleaning fields.

4. Conclusion: In summary, ultrathin ZnS nanobelts are successfully synthesised through simple CVD method. XRD characterisation shows that ZnS product possesses well-identified hexagonal wurtzite structure. A plausible growth mechanism of nucleation and oriental attachment for ZnS nanobelts is proposed. Characteristic peak of PL spectrum confirms the as-prepared ZnS product possesses some defects. CA photographs of ZnS nanobelts shows that the as-obtained ZnS nanobelts are hydrophobic with 113° contact angle, demonstrating its potential applications in self-clean fields.

5. Acknowledgments: This work was supported by initial funding for top level talents of the Shenyang University of Technology and Nature Science Fund of Liaoning province (grant no. 20170540671).

6 References

[1] Zhang Z.X., Wang J.X., Yuan H.J., *ET AL.*: 'Low-temperature growth and photoluminescence property of ZnS nanoribbons', *J. Phys. Chem. B*, 2005, **109**, pp. 18352–18355

[2] Jia W.N., Jia B.X., Wu X., *ET AL.*: 'Self assembly of shape-controlled ZnS nanostructures with novel yellow light photoluminescence and excellent hydrophobic properties', *CrystEngComm*, 2005, **14**, pp. 7759–7763

[3] Hu J.T., Wang G.Z., Guo C.X., *ET AL.*: 'Au-catalyst growth and photoluminescence of zinc-blende and wurtzite ZnS nanobelts via chemical vapor deposition', *J. Lumin.*, 2007, **122**, pp. 172–175

[4] Jia W.N., Wu X., Jia B.X., *ET AL.*: 'Self assembled porous ZnS nanospheres with high photocatalytic performance', *Sci. Adv. Mater.*, 2013, **5**, pp. 1329–1336

[5] Wu X., Qu F.Y., Shen G.Z., *ET AL.*: 'Large-scale synthesis of fishbone-like ZnS nanostructures using ITO glass as the substrate', *J. Alloy Compd.*, 2009, **482**, pp. L32–L35

[6] Wang X.D., Summers C.J., Wang Z.L.: 'Large-scale hexagonal-patterned growth of aligned ZnO nanorods for nano-optoelectronics and nanosensor arrays', *Nano Lett.*., 2004, **4**, pp. 423–426

[7] Jia W.N., Jia B.X., Lin H.M., *ET AL.*: 'Solution growth and optical property of ZnS/ZnO microspheres', *Micro Nano Lett.*, 2011, **6**, pp. 633–635

[8] Rashmi L., Bednarz B., Hackens G., *ET AL.*: 'Nonlinear electron transport properties of InAlAs/InGaAs based Y-branch junctions for microwave rectification at room temperature', *Solid State Commun.*., 2005, **134**, pp. 217–222

[9] Han Z.C., Zheng X., Hu F., *ET AL.*: 'Facile synthesis of hollow ZnS nanospheres for environmental remediation', *Mater. Lett.*, 2015, **160**, pp. 271–274

[10] Shen G.Z., Bando Y., Ye C.H., *ET AL.*: 'Single-crystal nanotubes of II_3–V_2 semiconductors', *Angew. Chem., Int. Ed.*, 2006, **45**, pp. 7568–7572

[11] Wu X., Lei Y., Zheng Y.F., *ET AL.*: 'Controlled growth and cathodoluminescence property of ZnS nanobelts with large aspect ratio', *Nano-Micro Lett.*, 2010, **2**, pp. 272–276

[12] Liu Y., Jiao Y., Zhang Z.L., *ET AL.*: 'Hierarchical SnO_2 nanostructures made of intermingled ultrathin nanosheets for environmental remediation, smart gas sensor and supercapacitor applications', *ACS Appl. Mater. Interfaces*, 2014, **6**, pp. 2174–2184

[13] Yao S.Y., Zheng X., Zhang X., *ET AL.*: 'Facile synthesis of flexible WO_3 nanofibers as supercapacitor electrodes', *Mater. Lett.*, 2017, **186**, pp. 94–97

[14] Gao L.N., Qu F.Y., Wu X.: 'Hierarchical WO_3@SnO_2 core/shell nanowire arrays on carbon cloth: a new class of anode for high performance lithium-ion batteries', *J. Mater. Chem. A*, 2014, **2**, pp. 7367–7372

[15] Lei Y., Qu F.Y., Wu X.: 'Assembling ZnO nanorods into microflowers through a facile solution strategy: morphology control and cathodoluminescence properties', *Nano-Micro Lett.*, 2012, **4**, pp. 45–51

[16] Wu X., Jiang P., Ding Y., *ET AL.*: 'Mismatch strain induced formation of ZnO/ZnS heterostructured rings', *Adv. Mater.*, 2007, **19**, pp. 2319–2323

[17] Li D., Medlin J. W.: 'Application of polymer-coated metal-insulator-semiconductor sensors for the detection of dissolved hydrogen', *Appl. Phys. Lett.*, 2006, **88**, p. 233507

[18] Liu Z., Yan P.X., Yue G.H., *ET AL.*: 'Red light photoluminescence emission from Mn and Cd co-doped ZnS one-dimensional nanostructures', *J. Phys. D, Appl. Phys.*, 2006, **39**, pp. 2352–2356

[19] Wang Z.L., Kong X.Y., Zuo J.M: 'Induced growth of asymmetric nanocantilever arrays on polar surfaces', *Phys. Rev. Lett.*, 2003, **91**, pp. 185502

[20] Feng X.J., Jiang L.: 'Design and creation of superwetting/antiwetting surfaces', *Adv. Mater.*, 2006, **18**, pp. 3063–3078